Running head: POLYGENIC RISK, NEURODEVELOPMENT AND RESILIENCE

Psychological Resilience in Adolescence as a function of Genetic Risk for Major Depressive Disorder and Alzheimer's Disease

Raluca Petrican[1*] and Alex Fornito[2]

[1]Cardiff University Brain Research Imaging Centre (CUBRIC), School of Psychology, Cardiff University, Maindy Road, Cardiff, CF24 4HQ, United Kingdom, email: petricanr@cardiff.ac.uk. [2]The Turner Institute for Brain and Mental Health, School of Psychological Sciences, and Monash Biomedical Imaging, Monash University, Melbourne, VIC, Australia., email: alex.fornito@monash.edu

[*]Corresponding author email address: petricanr@cardiff.ac.uk (R.P.).

Conflict of interest. The authors declare no competing interests.

Abstract

Major Depressive Disorder (MDD) and Alzheimer's Disease (AD) are two pathologies linked to prior stress exposure and altered neurodevelopmental trajectories. As a putative antecedent to AD, MDD could be key to understanding the neurobiological changes that precede the clinical onset of AD by decades. To test this hypothesis, we used longitudinal data from the Adolescent Brain and Cognitive Development study (N_{total} = 980, 470 females) and investigated overlapping connectomic, transcriptomic, and chemoarchitectural correlates of adjustment to stressors (i.e., resilience) among adolescents at genetic risk for AD and MDD, respectively. The potential for perinatal adversity to directly and/or indirectly, via accelerated biological ageing, foster resilience (i.e., "inoculation" effects) was also probed. We identified two distinguishable neurodevelopmental profiles predictive of resilience among MDD-vulnerable adolescents. One profile, expressed among the fastest developing youth, overlapped with areas of greater dopamine receptor density and reflected the maturational refinement of the inhibitory control architecture. The second profile distinguished resilient MDD-prone youth from psychologically vulnerable adolescents genetically predisposed towards AD. This profile, associated with elevated GABA, relative to glutamate, receptor density, captured the longitudinal refinement and increasing context specificity of incentive-related brain activations. Its transcriptomic signature implied that poorer resilience among AD-prone youth may be associated with greater expression of MDD-relevant genes. Our findings are compatible with the proposed role of MDD as a precursor to AD and underscore the pivotal contribution of incentive processing to this relationship. They further speak to the key neuromodulatory role of DA-gonadal hormone interactions in fostering resilience in adolescence.

Keywords*:* Psychological Resilience; Major Depressive Disorder; Alzheimer's Disease; Adolescent Development; Polygenic Risk; Transcriptomics.

Significance Statement

Environmental stressors can substantially alter brain maturation and incur lifelong costs. Using longitudinal data, we characterise two developmental profiles correlated with positive adjustment to environmental challenges (i.e., resilience) among adolescents at genetic risk for two stress-related conditions, Alzheimer's Disease (AD) and Major Depressive Disorder (MDD), respectively. One dopamine-related profile typified the fastest developing MDD-prone adolescents and reflected the neural maturation of the inhibitory control architecture. The second profile, neurochemically linked to excitation/inhibition balance, indicated the developmental refinement of motivational pathways, distinguishing resilient MDD-prone from psychologically vulnerable AD-prone teens. Its transcriptomic signature supported the posited role of MDD as an antecedent to AD. Our results unveil candidate neurobiological mechanisms supporting lifespan resilience against both psychiatric and neurological conditions linked to stress exposure.

Psychological Resilience in Adolescence as a function of Genetic Risk for Major Depressive Disorder and Alzheimer's Disease

Adolescence is a critical developmental phase, marked by a multitude of interdependent neurobiological and socio-environmental changes that are programmed to maximise adjustment to one's milieu (1,2). Unsurprisingly, this is also the life stage in which more than a third of all diagnosed mental disorders have their onset (3), a finding that underscores the urgency in comprehensively characterising the developmental markers of subsequent adaptation versus vulnerability (4, 5).

Alzheimer's Disease (AD) and Major Depressive Disorder (MDD) are two conditions typified by altered brain maturation/ageing trajectories, in part stemming from systemic inflammation processes (6-8). Robustly linked to greater stress susceptibility and exposure, as well as genes regulating lifespan neurodevelopment, the two disorders have been posited to share a causal connection, with MDD and broader predispositions towards experiencing negative affect being regarded as risk factors or even early symptoms of AD (9-14).

Although the clinical onset of AD occurs mid- to late adulthood, compelling evidence suggests that the preceding decades are marked by significant cellular changes linked to more subtle cognitive-behavioural markers (15). Given that AD-relevant genetic risk factors are under considerable environmental modulation (16), identification of early life neurodevelopmental alterations among vulnerable individuals could be instrumental in designing interventions to slow down or even prevent progression towards dementia.

Leveraging the purported relationships among stress, MDD and AD, we used a longitudinal design to probe the overlap of the macroscale (functional connectomic) and molecular (neurochemical and transcriptomic) brain correlates of psychological resilience

(i.e., positive adjustment to environmental challenges, [17, 18]) as a function of genetic risk for MDD versus AD. Overlapping substrates could unveil common pathways linking stress exposure to both AD and MDD, thereby justifying subsequent investigations into whether neurodevelopmental mechanisms that promote early life resilience may also foster resistance to AD in older adulthood.

Secondarily, we sought to extend findings on the lifelong neurodevelopmental consequences of perinatal adversity exposure by characterising its potential risk-enhancing or protective ("inoculation"-like) role with regards to resilience, whether manifest directly or indirectly via an altered rate of biological ageing (i.e., pubertal timing) (cf. 19-25). Our complete model is depicted in Figure 1.

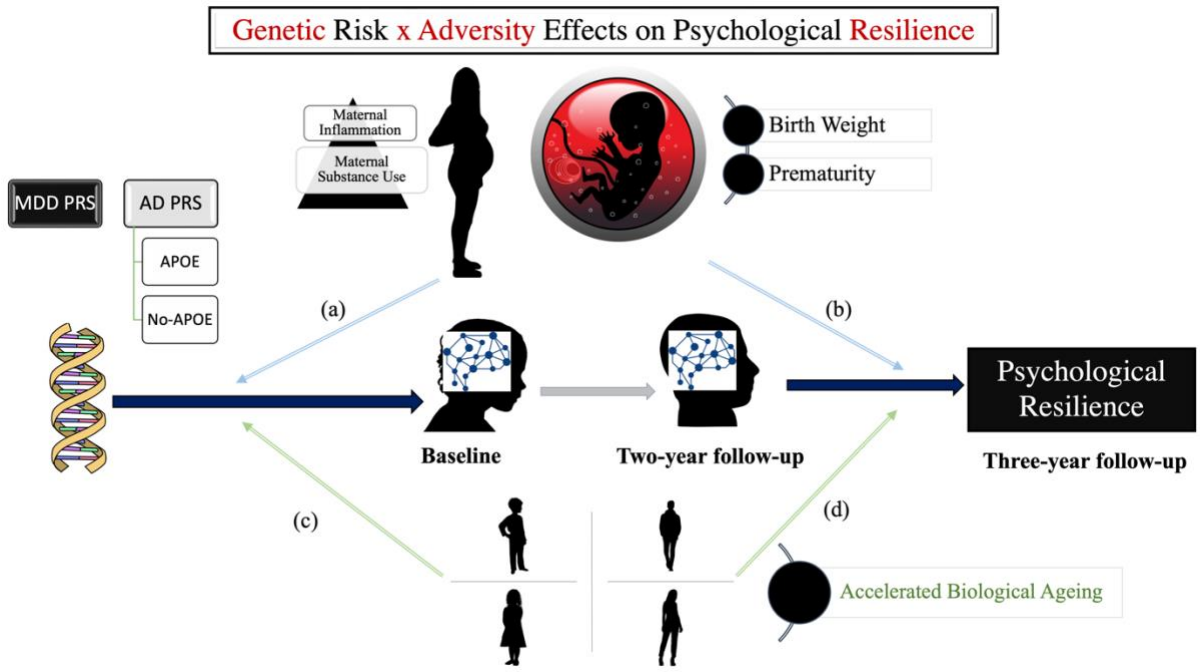

Figure 1. Schematic representation of the conceptual/measurement model. Genetic risk for AD (APOE vs no-APOE-based, see Method for details) and MDD, respectively, were predicted to impact functional brain maturation, specifically, longitudinal fine-tuning and contemporaneous, cross-context differentiation, as observed on inhibitory control and incentive processing tasks. The primary goal was to identify neurodevelopmental patterns that would alleviate the expected negative impact of AD/MDD genetic risk on resilience. The moderating, potentially protective ("inoculation"-like effect) effects of perinatal

adversity and accelerated biological ageing on gene-brain (paths a, c) and brain-resilience (paths b, d) were also probed.

In light of its well-demonstrated utility in modelling trajectories of both normative brain maturation and (transdiagnostic) pathology, including AD, a network neuroscience approach was applied to longitudinal multimodal data from the Adolescent Brain and Cognitive Development (ABCD) study (26-28). Genetic vulnerability to AD and MDD, respectively, was quantified using polygenic risk scores (PRS, [29]) derived from genome-wide association studies (GWAS) (30-31). Developmental connectomic correlates of resilience were estimated in reference to two mental processes, inhibitory control and reward processing, which change substantially in adolescence, are highly susceptible to adversity and predictive of subsequent (psycho)pathology, including later life vulnerability to dementia (32-38). Molecular correlates of resilience were quantified using group-based normative maps of gene expression and receptor density focused on four neutransmitters (dopamine [DA], serotonin [5-HT], glutamate [GLU], gamma-aminobutyric acid [GABA]) implicated in cognitive control, incentive processing, susceptibility to stress/resilience, as well as AD/MDD vulnerability, more specifically (39-49).

Results

Mesoscale Functional Brain Correlates of Resilience and AD/MDD Risk

To characterise functional connectomic features linked to resilience, we applied a network-based clustering technique, referred to as “multilayer community detection” (50) to fMRI data collected during two tasks assessing inhitory control and incentive processing, respectively (26). Using the Schaefer 300 parcel-functional atlas (51) and the “flexibility” function from the Network Community Toolbox (52), we estimated longitudinal (baseline-to-2-year follow-up) within-task and cross-task (inhihibitory control/incentive processing) contemporaneous differences in functional brain architecture (i.e., changes in each parcel’s

functional community assignment [53]). The first index gauged fine-tuning of task-specific functional brain architecture. The second index reflected context-specificity in neural coding (i.e., inhibitory control-incentive processing differentiation), a cross-species marker of adaptive functioning and resilience (54-56). Partial least squares analysis (PLS) was subsequently applied to parcel-specific "flexibility" indices to identify connectomic features linked to resilience and/or genetic risk for AD/MDD.

PLS analysis 1 identified two latent variables (LVs, *p*-values of .0002 and .001, respectively), which accounted for 18.20% and 12.83%, respectively, of the brain-behaviour covariance. The first extracted LV related greater MDD risk, accelerated biological ageing and resilience to longitudinal increases in Control, somatomotor (SM), Salience/Ventral Attention (SAL/VAN), default mode (DMN) and visual (VIS) functional reconfiguration on the inhibitory control task (see Figure 2-a, b). The second LV linked VIS-related longitudinal and cross-task functional reorganisation at follow-up to higher resilience in the presence of stronger MDD, but weaker AD, risk (see Figure 3-a, b). Specifically, it implied that psychological health may hinge on refinement of VIS responses to incentives and rising task-specificity in processing.

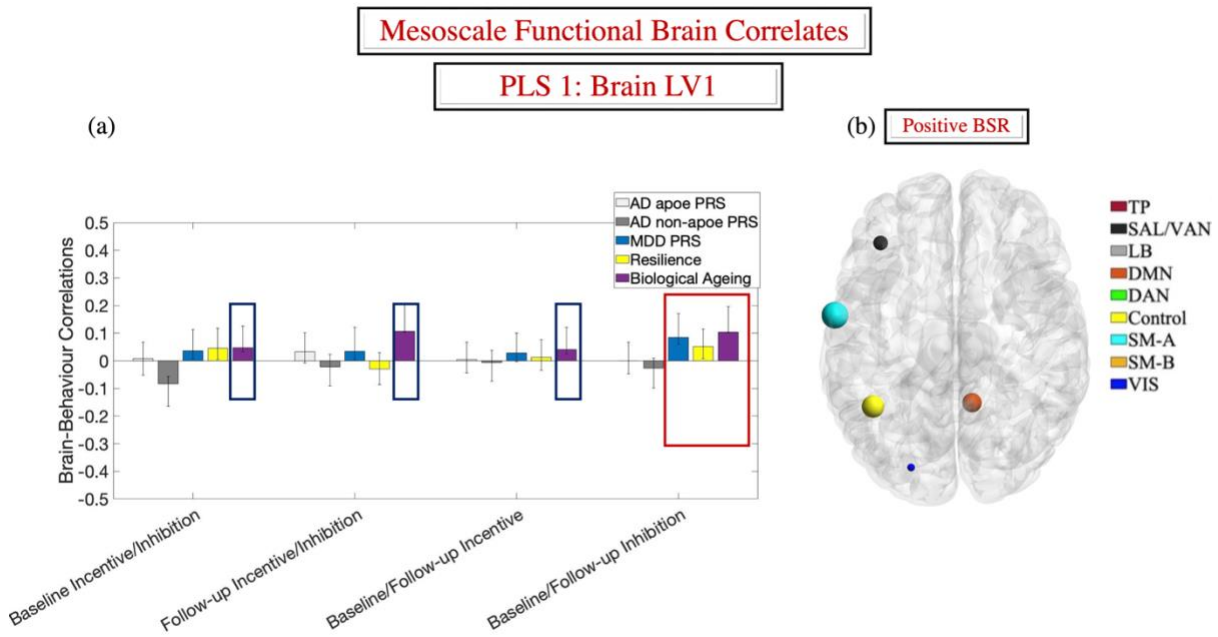

Figure 2. First extracted LV from the behavioral-PLS analysis linking AD/MDD genetic risk, resilience, and biological ageing to longitudinal and contemporaneous cross-context differentiation of the functional brain architecture relevant to incentive processing vs inhibitory control. Panel (a) shows the correlations between the behavioral variables and the brain scores in each condition. Panel (b) depicts the Schaefer parcels with robust loadings (absolute value BSR > 3) on the LV in panel (a) and visualized with the BrainNet Viewer (http://www.nitrc.org/projects/bnv/) (Xia et al., 2013). Parcel colours reflect Schaefer et al.'s network assignments. In panel (b), the size of the parcels is proportional to their associated absolute value BSR. Error bars are the 95% confidence intervals from the bootstrap procedure. Confidence intervals that do not include zero reflect robust correlations between the respective behavioral variable and the brain score in a given condition across all participants. In panel (a), hypothesis-relevant, significant brain-behavior correlations, replicated across all the supplemental analyses, are within red line rectangles. Significant brain-behavior correlations unrelated to our hypotheses are in blue rectangles. All the reported PLS analyses had been conducted on parcel-specific indices. Network labels attached to the parcels are included for informational purposes only. LV= latent variable. PRS = polygenic risk score. BSR = bootstrap ratio. Schaefer networks: TP= temporo-parietal. SAL-VAN = salience/ventral attention. LB = limbic. DMN = default mode. DAN = dorsal attention. SM-A =somatomotor-A. SM-B =somatomotor-B. VIS = visual.

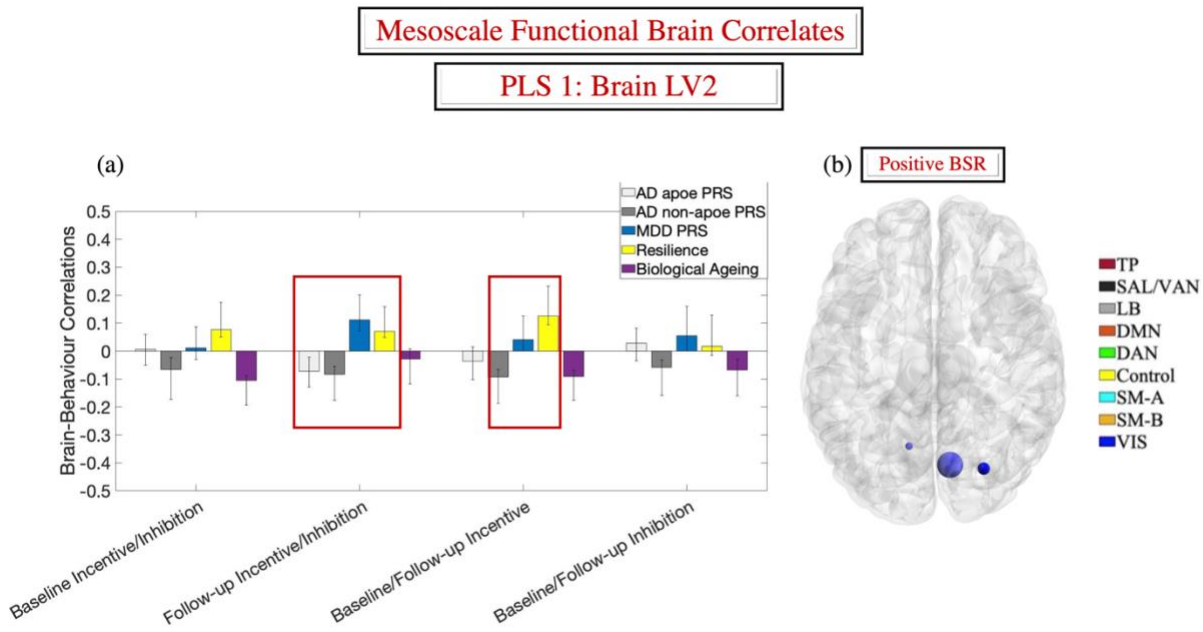

Figure 3. Second extracted LV from the behavioral-PLS analysis linking AD/MDD genetic risk, resilience, and biological ageing to longitudinal and contemporaneous cross-context differentiation of the functional brain architecture relevant to incentive processing vs inhibitory control. Panel (a) shows the correlations between the behavioral variables and the brain scores in each condition. Panel (b) depicts the Schaefer parcels with robust loadings (absolute value BSR > 3) on the LV in panel (a) and visualized with the BrainNet Viewer (http://www.nitrc.org/projects/bnv/) (Xia et al., 2013). Parcel colours reflect Schaefer et al.'s network assignments. In panel (b), the size of the parcels is proportional to their associated absolute value BSR. Error bars are the 95% confidence intervals from the bootstrap procedure. Confidence intervals that do not include zero reflect robust correlations between the respective behavioral variable and the brain score in a given condition across all participants. In panel (a), hypothesis-relevant, significant brain-behavior correlations replicated across all the supplemental analyses, are within red line rectangles. Significant brain-behavior correlations unrelated to our hypotheses are in blue rectangles. All the reported PLS analyses had been conducted on parcel-specific indices. Network labels attached to the parcels are included for informational purposes only. LV= latent variable. PRS = polygenic risk score. BSR = bootstrap ratio. Schaefer networks: TP= temporo-parietal. SAL-VAN = salience/ventral attention. LB = limbic. DMN = default mode. DAN = dorsal attention. SM-A =somatomotor-A. SM-B =somatomotor-B. VIS = visual.

The above PLS results were replicated with a distinct functional brain atlas (see Supplemental Materials). Exploratory PLS analyses conducted with males and females as two separate groups did not reveal any reliable sex differences with regards to the connectomic correlates of resilience or AD/MDD genetic vulnerability.

Microscale Correlates of Resilience and AD/MDD Risk

To characterise the transcriptomic signature of the two brain LVs described above, we used the abagen toolbox (57) and quantified gene expression levels in each of the Schaefer parcels (see *Methods*). Two PLS analyses were subsequently conducted on the resilience-relevant brain LVs and the parcel x gene matrices outputted by the abagen toolbox.

Gene-brain PLS 1: Left-hemisphere only. The gene-brain PLS analysis identified a sole LV (p = .017), which accounted for 70% of the brain-gene covariance. The extracted gene LV was positively correlated with both the brain LV1 (cf. Figure 2), r = .32, 95% CI = [.25; .45] and brain LV2 (cf. Figure 3), r = .48, 95% CI = [.40; .62].

Gene-brain PLS 2: Bi-hemispheric. The above brain-gene pattern was replicated using the bi-hemispheric gene expression data from the Schaefer atlas (p = .017, 63% brain-gene covariance explained; see Figure 4-a, b for the spatial expression profile of the gene LV). As expected, the identified gene LV was robustly related to both brain LVs (LV1: r = .30, 95%CI = [.24; .39]; LV2: r = .42, 95%CI = [.36; .51]).

MDD-relevant gene expression profile. To test whether the neural markers of genetic risk for AD are linked to greater expression of MDD-relevant genes in adolescence, consistent with MDD as a precursor to AD proposal, we used the expression quantitative trait locus (eQTL) analysis data from the MDD GWAS conducted by [31]. The MDD-relevant candidate risk loci had been mapped onto the corresponding genes by the original authors using the SNP2GENE tool in FUMA and made available via the Public Results tab (https://fuma.ctglab.nl/browse). Based on their eQTL analysis output, we identified 156

MDD-linked genes reliably expressed in our data. Of these, the risk allele(s) reduced gene expression for 76 of them (MDD_low), but increased gene expression for the remaining 80 (MDD_high).

To characterise the transcriptomic signature of resilience and AD/MDD genetic risk, we focused on genes with an absolute value BSR of at least 4 (associated p-value < 10^{-4}) in the brain-gene PLS analyses described above. Based on the brain-gene LV correlations, MDD-relevant transcriptomic associations with resilience, accelerated biological ageing and higher MDD PRS were derived from the number of MDD_low genes with negative BSRs and MDD_high genes with positive BSRs. Complementarily, the number of the MDD_high genes with negative BSRs and MDD_low genes with positive BSRs was used to test for an association between higher no-APOE-based AD PRS (see Figure 3-a) and stronger expression of the MDD-relevant gene expression profile.

No significant association was detected between the MDD-relevant gene expression and the resilience-linked brain LVs (*p*-values of .08 and .69 based on left hemisphere and bi-hemispheric data, respectively). In contrast, we found evidence of a significant relationship between the MDD-relevant transcriptomic profile and the neurodevelopmental profile yoked to no-APOE-based genetic risk for AD (*p*-values of .037 and .010 based on left hemisphere and bi-hemispheric data, respectively; for relative MDD gene contribution, see Figure 4-c, d).

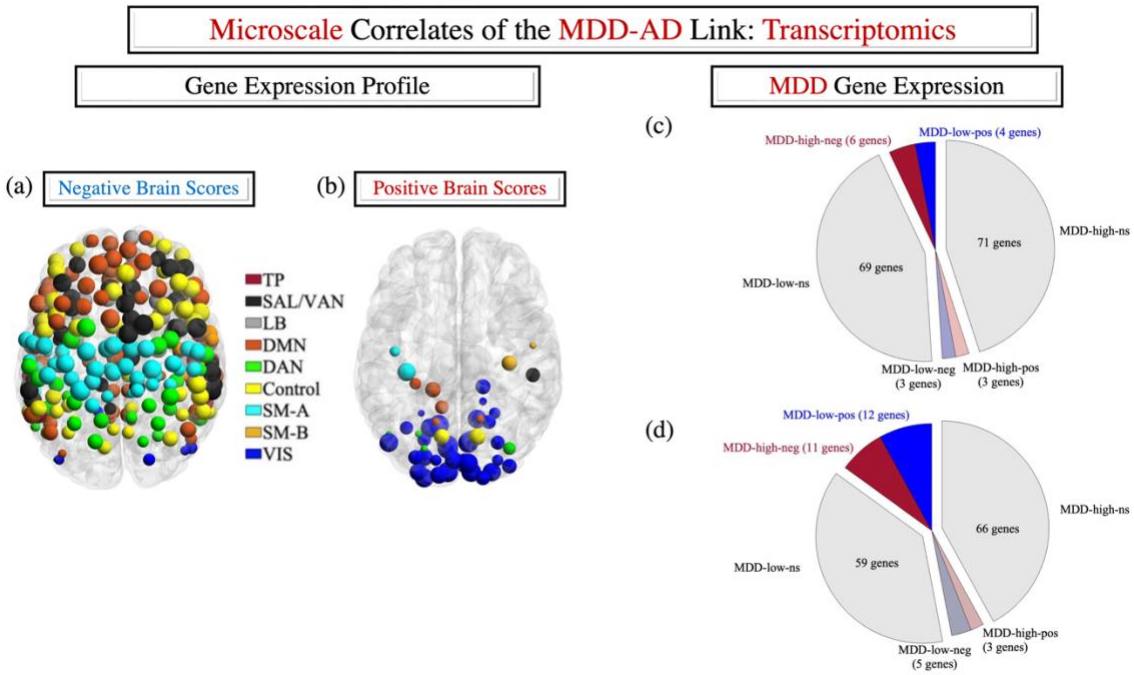

Figure 4. Transcriptomic correlates of the AD-MDD link. Panels (a) and (b) represent the spatial expression map of the gene LV identified in the gene-brain behavioral PLS analysis. The parcels were visualized with the BrainNet Viewer (http://www.nitrc.org/projects/bnv/) (Xia et al., 2013). Parcel colours reflect Schaefer et al.'s network assignments and their size is proportional to how strongly they express the gene LV (i.e., the absolute value of the associated brain score). Panels (c) and (d) depict the results of the MDD/no-APOE AD PRS overlap analyses, using only left-hemisphere (c) or bi-hemispheric (d) data. As described in the text, these are based on the gene LV depicted in panels (a) and (b), which was negatively correlated with the no-APOE PRS (see Figure 3-a). LV= latent variable. BSR = bootstrap ratio. Schaefer networks: TP= temporo-parietal. SAL-VAN = salience/ventral attention. LB = limbic. DMN = default mode. DAN = dorsal attention. SM-A =somatomotor-A. SM-B =somatomotor-B. VIS = visual.

Receptor density maps. To elucidate the overlap between our two resilience-relevant brain profiles and density maps of neurotransmitters which play a substantial role in psychopathology (GLU/GABA [E/I], DA [combined D1/D2], HT), we used the normative group-based atlas provided by [58] and conducted a series of partial correlation analyses with permutation-based significance testing featuring 100,000 spatially constrained null brain maps [59].We thus correlated each of the two brain LVs with each of the three density maps

controlling for the remaining maps (e.g., correlate brain LV1 with the combined D1/D2 receptor density map, while controlling for HT, GABA and GLU receptor densities). We identified two significant correlations replicated with a second functional atlas (see Supplemental Materials). Specifically, brain LV1 demonstrated a significant association with the DA (combined D1/D2) receptor density map (*r* of .20, spin test *p* = .046), while brain LV2 showed a significant negative correlation with the E/I density map (*r* of -.40, spin test *p* = .002) (see Figure 5-a, d for the scatter plots describing these relationships and Figure 5-b, c, e for the E/I and DA receptor density maps).

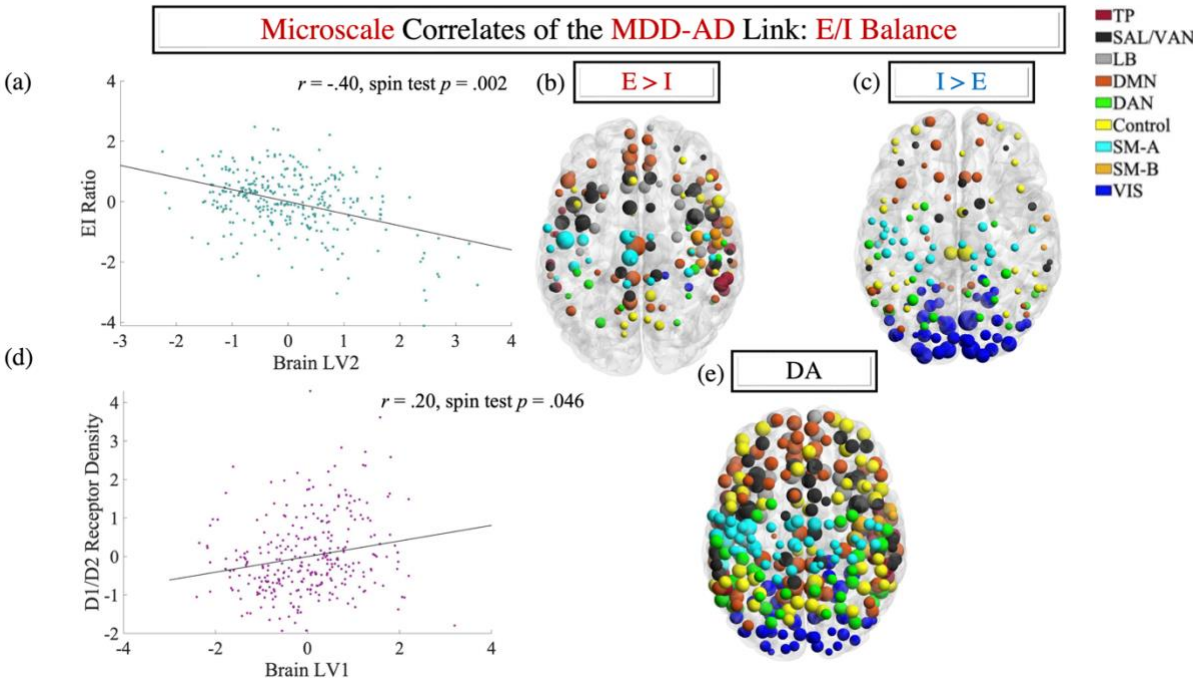

Figure 5. Results of the correlational analyses linking the E/I and DA receptor density map to the two brain LVs relevant to AD/MDD genetic risk, resilience and biological ageing (see Figures 2 and 3). Panels (a) and (d) contain the scatter plots describing the linear relationship between brain LV2 and the E/I (GLU/GABA) density map (a), as well as between brain LV1 and the DA density map. Panels (b) and (c) represent the areas of E > I density and I > E density, respectively, whereas panel (e) depicts the DA receptor density map. The parcels were visualized with the BrainNet Viewer (http://www.nitrc.org/projects/bnv/) (Xia et al., 2013). Parcel colours reflect Schaefer et al.'s network assignments and their size is proportional to the density of the respective receptor. E/I = excitation/inhibition. GLU = glutamate. GABA = gamma-aminobutyric acid. DA = dopamine.

Perinatal adversity and accelerated biological ageing as moderators of the AD/MDD genetic risk-resilience relationship

Finally, we examined the role of perinatal adversity and accelerated biological ageing in modulating the impact of AD (no-APOE-based, see Figure 3-a) and/or MDD (see Figures 2-, 3-a) genetic risk on psychological resilience at the three-year follow-up. To this end, we specified the two moderated parallel mediator models conceptually represented in Figure 1. The LV2 scores in the "Follow-up Incentive/Inhibition" and "Baseline/Follow-up Incentive" conditions were robustly correlated (r =.43, p < .001). Consequently, in the absence of condition-specific predictions, the LV2 scores corresponding to the aforementioned conditions were standardised across participants and then averaged. The inhibition-linked LV1 (see Figure 2-a) and the averaged LV2 score were introduced as mediators. For the purpose of these analyses, the biological ageing variable was binned into "Low" (lowest 50% developing participants) and "High" (fastest 50% developing participants).

Accelerated biological ageing strengthens the link between genetic risk for MDD and neurodevelopmental patterns predictive of subsequent resilience. Of the two partial moderated mediation models tested, only one emerged as significant, with an index of .014, SE = .008, 95% CI [.002; .032]. Specifically, we found that brain LV1 scores were predicted by a robust MDD PRS x biological ageing interaction, b = .161, SE = .064, t(974) = 2.510, p = .012 (see Figure 6-b), such that the link between the brain LV1 and MDD PRS was significant among the fastest developing participants, effect of .168, SE = .046, 95% CI [.078; .257]. Accordingly, follow-up analyses confirmed that a significant mediation of MDD PRS effects on resilience via the brain LV1 was observed only for participants showing faster biological ageing, effect of .015, SE = .007, 95% CI [.003; .030].

Simple mediation models. Two follow-up parallel mediator models revealed that brain LV2 partially explained the indirect effect (IE) of no-APOE-based AD vulnerability on

reduced resilience, IE = -.016, SE = .006, 95% CI [-.029; -.005] (see Figure 6-a), as well as the association between the MDD PRS and greater resilience, IE = .014, SE = .006, 95% CI [.004; .027] (see Figure 6-b).

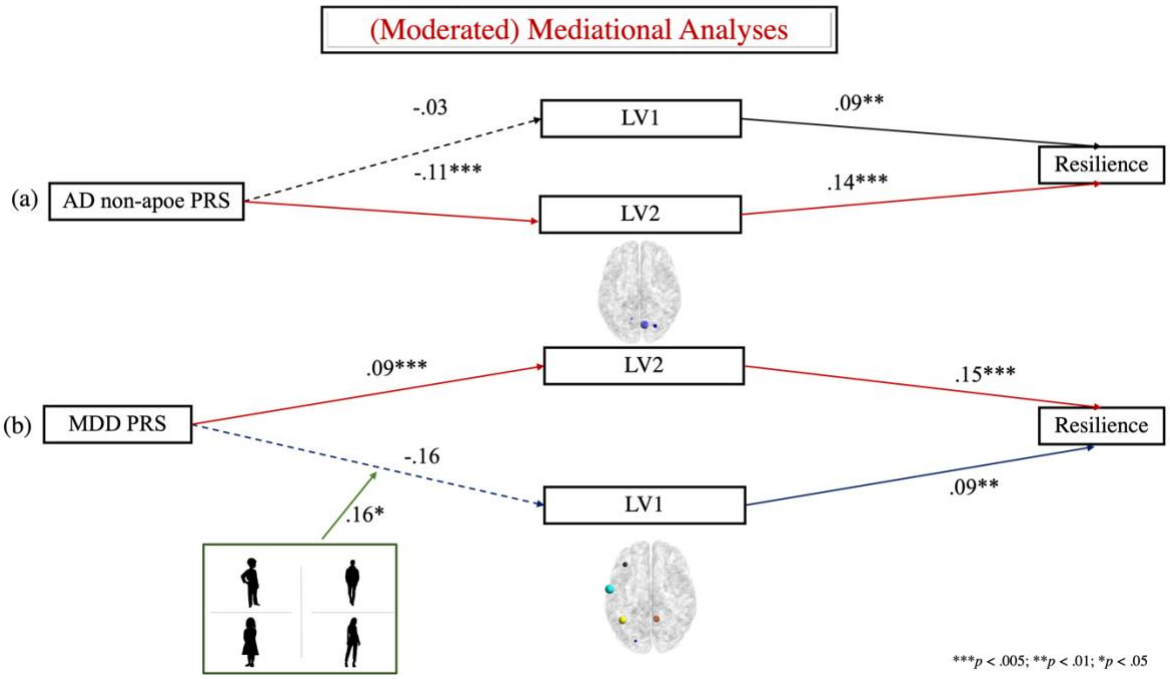

Figure 6. (Moderated) mediational models linking genetic vulnerability to AD (panel a) and MDD (panel b), respectively to psychological resilience as assessed at the three-year follow-up. In both panels, the coefficients associated with the red paths had been derived from simple mediational analyses (as described in the text). The coefficients associated with the blue paths are based on the moderated mediation analyses. A dashed line indicates a statistically non-significant path ($p > .05$).

Discussion

Applying a multidimensional approach to longitudinal data from the ABCD study, we provide novel evidence of two neurodevelopmental profiles predictive of positive adjustment to environmental challenges as a function of genetic liability to AD/MDD. One profile reflected the brain mechanisms recruited by resilient adolescents who are at risk for MDD. Reinforcing the contribution of DA to both cognitive control and resilience (42, 47, 60), this profile captured the longitudinal fine-tuning of the inhibitory control architecture, spanning

areas of greater DA receptor density in functional systems that are trans-diagnostically involved in psychopathology (SAL, SM, DMN, Control, 36, 61, 62). Of note, the protective effects of this brain profile were strongest among the fastest maturing adolescents (i.e., those showing higher pubertal hormone levels), in line with prior demonstrations of DA-mediated gonadal hormone effects on behaviour, including liability to MDD (63-65). More broadly, this profile speaks to the value of longitudinal investigations of DA-gonadal hormone (particularly estradiol) dynamics in uncovering fluctuating substrates of resilience as a function of adversity exposure and differential gene expression patterns, including those observed across the various menstrual cycle stages (63, 66, 67).

A second neurodevelopmental profile differentiated resilient youth at genetic risk for MDD from psychologically vulnerable adolescents genetically predisposed towards AD. Longitudinal fine-tuning and cross-context differentiation of the neural architecture underpinning incentive processing emerged as a key resilience-promoting mechanism among the MDD-vulnerable youth. Conversely, network rigidity related to poorer resilience among AD-prone adolescents. Anchored in VIS areas of greater GABA, relative to GLU, receptor density, this profile reaffirmed the importance of externally oriented processing systems to MDD pathology (e.g., [68]), as well as the role of E/I balance in supporting functional network development (69). It also underscored the importance of conducting more targeted, neurotransmitter system-specific investigations into the relationships among AD/MDD risk, resilience and incentive processing. For instance, distinguishable GLU neuron populations in the ventral tegmental area (VTA) have been implicated in coding rewards and losses (70), while GABA and GLU neurons in the basal ganglia have been shown to code for rewards and threats, respectively (71, 72). Extending these findings, it would be worth establishing whether the observed E/I link to resilience in MDD- vs AD-predisposed individuals manifests through distinguishable pathways (e.g., threat/loss- vs reward-linked). Such a line

of inquiry would be well-served by studies targeting neurotransmitter-specific substrates of whole-brain functional network interactions, while accounting for age-related modulation (73), including effective connectivity patterns between subcortical and cortical regions. This work would further benefit from experimental manipulations targeting the variety of mental processes (e.g., positive emotion upregulation vs negative emotion downregulation, 74) and cells-to-networks neurobiological mechanisms underlying resilience as a function of stressor and genetic vulnerability.

Finally, we also found evidence compatible with the putative causal role of MDD in later AD onset (10, 13). Specifically, our results raised the possibility that lower resilience among adolescents at risk for AD may stem (partly) from poorer fine-tuning of the incentive processing architecture, linked to stronger expression of MDD-relevant risk genes. As our neurodevelopmental findings centered around VIS areas, implicated in episodic memory (re)construction processes (75, 76), they are well-aligned with recent proposals on the role of episodic memory in partially explaining the link between MDD and AD genetic risk (13).

Broadly, our present findings call for more fine-grained investigations of candidate neurobiological mechanisms underpinning the link between MDD and AD. Inflammatory processes linked to hypothalamic-pituitary-adrenal (HPA) axis dysregulation (10) would warrant special attention, particularly zooming in on alterations observed in astrocytes, microglia and mitochondria, given their susceptibility to stress, E/I modulation, as well as role in neurodegeneration and psychological resilience (77-82).

Limitations and Future Directions

Our present research opens several new avenues of inquiry. First, there is suggestive evidence that, compared to traditional laboratory tasks (such as those used in the ABCD study), naturalistic paradigms may yield neurocognitive patterns that better resemble those likely to be evoked in real-world settings (83). Consequently, replication and extension of our

findings in studies featuring a movie watching paradigm, for instance, could yield further insights into the results herein documented. Second, patterns of functional network interactions underpinning optimal adjustment have been shown to vary by domain (i.e., cognition, personality, mental health) (84). As such, key insights could be gained by further probing our present findings on resilience through investigations on the neurodevelopmental mechanisms underpinning AD/MDD genetic risk and adaptive profile of cognition and/or personality.

Third, stronger genetic effects are reportedly observed on structural (relative to functional) brain indices, while structure-function coupling in connectomic features is also under substantial genetic modulation (85). Consequently, investigations of synchronised structure-function development would augment the findings herein reported, particularly given the robust predictive power of both white and gray matter indices for AD and MDD, as well as psychological resilience (86-88).

Fourth, while we provided suggestive evidence on the chemoarchitectural correlates of resilience, further cross-species investigations probing specific receptor types (e.g., D1 vs D2, 89), as well as interactions among multiple neurotransmitter systems (cf. 90) within an experimental paradigm would provide a finer grained dynamic representation of the multiscale interactions underpinning resilience. Fifth, the reliable sex differences observed in stress responses (91, 92), as well as in the genetic architecture underlying complex traits (93), highlight the need for cross-species comparative research to characterise sex-specific neurogenetic substrates of resilience, including compensatory mechanisms linked to AD/MDD vulnerability.

Finally, there is a strong need for further investigation of the mechanisms underlying the resilience-promoting effects of lifestyle choices (e.g., aerobic exercise, 94) and social relationships, including parental and peer presence in earlier life (95, 96). In particular, cross-

368 species studies of neuroplasticity-mediated increases in resilience (97) may play a key role in
369 designing earlier life interventions to decelerate or annihilate progression towards dementia
370 in older adulthood.

371 **Conclusions**

372 Distinguishable neurodevelopmental profiles, reflecting fine-tuning of the inhibitory
373 control (accelerated biological ageing/DA-linked) vs incentive processing (E/I-related)
374 architecture, predicted resilience among MDD-vulnerable adolescents. Promising support
375 emerged for the proposed role of MDD as an early life precursor to AD, as poorer resilience
376 among AD-vulnerable youth was associated with an MDD-relevant transcriptomic signature.

377 **Methods**

378 **Participants**

379 The sample included biological parents and offspring who participated in the ongoing
380 Adolescent Brain Cognitive Development (ABCD) study. The analyses were based on data
381 from Caucasian participants only because most polygenic risk markers to date have been
382 based on this population and there is some evidence that genetic architecture and risk loci
383 may show some racial differences (98, 99).

384 The present research uses baseline, two-, and three-year follow-up data downloaded
385 in November 2021 as part of the ABCD Study Curated Annual Release 4.0 (https://data-
386 archive.nimh.nih.gov/abcd). Following the recommendations of the ABCD study team (as
387 detailed in the "abcd_imgincl01" file included in the data release), 980 Caucasian participants
388 (470 female), the majority of whom were predominantly right-handed (N = 814), were
389 selected on the basis of being biologically unrelated and having contributed high-quality data
390 on all measures of interest. At baseline, participants were aged 9-10 years (M = 119.97
391 months, SD = 7.40 months). Follow-up sessions were similarly spaced across participants

(baseline to two-year follow-up: M = 23.93 months, SD = 1.49 months; two- to three-year follow-up: M = 11.20 months, SD = 1.95 months).

Psychological Resilience

Participants' psychological resilience at the three-year follow-up was quantified by regressing out lifetime history of adverse experiences from the general psychopathology risk index (100, 101) multiplied by -1. Positive and negative residuals indicate greater and poorer resilience, respectively, relative to the sample mean (i.e., better- vs. worse-than-expected psychological functioning given experienced adversity).

Perinatal Adversity

An index of perinatal adversity was extracted through principal components analysis from caregiver responses on the Developmental History Questionnaire (100), which was completed at baseline. This summary score, available in the ABCD 4.0 Data Release, reflects maternal prenatal care, maternal substance use during pregnancy, prenatal maternal health conditions, prematurity, birth complications and developmental milestones. The scores released by the ABCD team were multiplied by (-1), so that higher positive values would indicate greater perinatal adversity. For the purpose of our analyses, these transformed scores were subsequently binned into "Low" (lowest 50% values) and "High" (highest 50% values).

Biological Ageing: Pubertal Timing

Parent ratings of pubertal development were selected as a measure of biological ageing due to their significant correlation with other indices of pubertal maturation. To create a more stable index of biological ageing, we averaged parent-rated pubertal development at baseline and the two-year follow-up (r of .65 [$p < .001$], Cronbach's alphas of .62 and .83). While this approach to estimating biological ageing was favoured for psychometric reasons, we verified its convergence with measures of pubertal hormones, such as the dehydroepiandrosterone (DHEA), estradiol and testosterone among those participants who

had both types of measures. An index of accelerated pubertal development was computed by regressing from the averaged pubertal development score the youth's chronological age (see section on residualisation below for further details), such that a positive residual score indicated accelerated biological ageing.

Functional Brain Architecture

Neurodevelopmental profiles relevant to inhibitory control and reward processing, respectively, were estimated during the in-scanner performance of a Stop Signal (SST) and monetary incentive delay (MID) task, respectively (26).

MRI data acquisition and preprocessing. Acquisition parameters and preprocessing steps for the ABCD study data are described in [102]. Our analyses used minimally preprocessed fMRI data available as part of the ABCD Study Curated Annual Release 4.0. The minimal preprocessing pipeline involved correction for head motion spatial and gradient distortions, bias field removal, and co-registration of the functional images to the participant's T1– weighted structural image. We further applied the following steps: (1) elimination of initial volumes (8 volumes [Siemens, Philips], 5 volumes [GE DV25], 16 volumes [GE DV26] to allow the MR signal to reach steady state equilibrium, (2) linear regression-based removal of quadratic trends and 24 motion terms (i.e., the six motion parameters, their first derivatives, and squares, cf. 151) from each voxel's time course.

Parcel definition. Our main analyses were based on the Schaefer 300 parcel-functional atlas (51), downloaded from https://github.com/ThomasYeoLab/CBIG. The atlas version we used encompasses 17 functional networks, spanning core systems, such as the DMN (A/B/C), Control (A/B/C), Salience/Ventral Attention (A/B), Dorsal Attention (DAN A/B), Somatomotor (SM A/B), Visual (VIS Central/Peripheral), Limbic (LB A/B), and Temporo-parietal (TP). The Schaefer atlas was available in the Montreal Neurological Institute (MNI) standard space. To align it with the participants' native space for each of the

four tasks (SST at Time 1/Time 2, MID at Time 1/Time 2), the following steps were implemented in FSL: (1) the middle image in each task run was converted to the MNI space (via the MNI-152 brain template available in FSL) and the inverse transformation (MNI-to-participant native space) was estimated; (2) the inverse transformation was used to align the Schaefer atlas to each participant's functional images, separately for each task run (SST at Time 1/Time 2, MID at Time 1/Time 2).

Parcel-to-parcel correlations in timeseries. Pairwise Pearson's correlations between all the Schaefer parcels were computed separately for the SST and MID in Matlab and expressed as Fisher's z-transformed scores. Because the two tasks are very similar in duration, we used all available data from each. Similar to prior studies using multilayer community detection algorithms (e.g., 53), only the positive Fisher's z-scores were entered in the network-level analyses detailed below, while negative z-scores were set to zero.

Network-level analyses. All the network-level metrics were computed using the Network Community Toolbox (52), as described below. Patterns of parcel-based functional reorganisation, longitudinally within each task and between the two tasks at the same time point were characterised with a multilayer generalised Louvain-like community detection algorithm implemented in the NCT. In line with extant practices (53), the spatial resolution parameter was set to the default value of 1. Taking our cue from other investigations of heterogenous mental states (53), we set to 0.5 the cross-layer (MID-SST at Time 1; MID-SST at Time 2; Time 1-to-Time 2 MID; Time 1-to-Time 2 SST) connection strength parameter. To account for the near degeneracy of the modularity landscape, the multilayer community detection algorithm was initiated 100 times and all the functional network interactions indices detailed below were averaged across all iterations.

Functional network development. Longitudinal (baseline-to-2-year follow-up) within-task and cross-task (SST/MID) contemporaneous differences in functional brain

467 architecture were estimated across all the modularity optimisation iterations. Specifically,
468 using the "flexibility" function in NCT, we quantified the number of times each parcel in the
469 Schaefer atlas changed communities between the two tasks at each wave and, within each
470 task, from baseline to follow-up.

471 **Polygenic Risk Scores (PRS)**

472 MDD and AD PRSs were each computed as the weighted sum of risk alleles based on
473 the summary statistics of two large GWASs focused on each disorder (30, 31, for AD and
474 MDD, respectively). We focused on these two GWASs for the following reasons: (1) public
475 availability of eQTL analysis output; (2) match to our Caucasian-only sample with [31] in
476 particular, being the largest MDD GWAS to date of this population; (3) use of clinical
477 diagnosis-based patient cases and, for [30] confirmed clinical cases of late-onset sporadic
478 AD, which would ease the interpretation of the derived PRSs and associated findings.

479 For AD, we computed a separate APOE region (chromosome 19:44.4-46.5 Mb)- vs
480 no-APOE region PRS because the two PRSs forecast distinguishable trajectories of
481 neurocognitive impairments and differential susceptibility to environmental factors (16). For
482 MDD, we used the the top 10k most informative variants, based on approximately 76k
483 patients and 230k controls, which had been made publicly available by [31]. These variants
484 had been obtained by clumping the corrsponding GWAS statistics with the following
485 parameters p1 = p2 = 1, window size < 500kb, and $r^2 > 0.1$.

486 Prior to PRS computation, the following preprocessing steps were implemented: (1)
487 genes with a minor allele frequency (MAF) < .05, insertion/deletion and ambiguous single
488 nucleotide polymorphisms (SNPs) (i.e., A/T and G/C pairs) were excluded; (2) highly
489 correlated SNPs ($r^2 > .10$) within a 500 kb window were eliminated. The SNPs which
490 survived the preprocessing and had an associated GWAS level $p \leq 5x10^{-8}$ contributed to the
491 computation of the disorder-specific PRSs (MDD PRS: N = 8 SNPs; no-APOE AD PRS: N =

10 SNPs; APOE AD PRS = 14 SNPs). In our main analyses we opted to use a stringent *p*-value (i.e., GWAS-level significant at $p < .05$) in order to identify the variants contributing most robustly to predicting genetic risk for AD/MDD. However, in supplemental analyses, we confirmed that the identified brain patterns linked to AD/MDD risk and resilience also emerged when using more lenient *p*-thresholds (see Figures S3-6).

Gene expression data processing and analysis

Microarray gene expression. Micro-array gene expression data were obtained from six postmortem brains (1 female, ages 24.0–57.0, 42.50 +/- 13.38) provided by the Allen Institute for Brain Science (https://www.brain-map.org/). Because all six brains had left hemisphere data, but only two brains contained data from the right hemisphere, our gene-brain analyses focused on the left hemisphere parcels. However, consistent with observations that gene expression patterns are largely symmetric across the two hemispheres, we provide evidence that our results are replicated when using gene expression patterns mirrored across the two hemispheres.

The gene expression data was processed with abagen (https://github.com/netneurolab/abagen), following the steps outlined in [57]. The resulting gene expression matrices, used in all our analyses, were in the format 297 (bilateral)/147 (left-hemisphere) (parcels) x 15,632 (genes). A list of parcels lacking reliable gene expression is included in the Supplemental Materials (Table S1).

MDD overlap tests. To test whether the neural markers of genetic risk for AD are linked to greater expression of MDD-relevant genes in adolescence, consistent with MDD as a precursor to AD proposal, we used the eQTL analysis data from the MDD GWAS conducted by [31]. The MDD-relevant candidate risk loci had been mapped onto the corresponding genes by the original authors using the SNP2GENE tool in FUMA and made available via the Public Results tab (https://fuma.ctglab.nl/browse). Based on their eQTL

analysis output, we identified 156 MDD-linked genes reliably expressed in our data. Of these, the risk allele(s) reduced gene expression for 76 of them (MDD_low), but increased gene expression for the remaining 80 (MDD_high).

To characterise the transcriptomic signature of resilience and AD/MDD genetic risk, we focused on genes with an absolute value BSR of at least 4 (associated p-value < 10^{-4}) in the brain-gene PLS analyses. Comparisons were conducted separately for genes with positive versus negative loadings on the gene LV. As an example, for the positive BSR genes, the procedure was as follows: (1) we obtained separate counts of the number of MDD_low and MDD_high genes, respectively, with a BSR of at least 4 on our gene LV (MDD_low_pos and MDD_high_pos, respectively); (2) we counted the number of genes with a BSR of at least 4 on our gene LV (Orig_pos); (3) from each of the corresponding gene LVs in the null distribution (each of which had been aligned with the original gene LVs via a Procrustes transform), we selected a number of genes equal to Orig_pos (Null_pos); (4) we counted the number of null samples (out of the total of 100,000) in which the number of either MDD_low_pos or MDD_high_pos in Null_Pos exceeded the one observed in Orig_pos. The same procedure was followed for the negative BSR genes. Estimation of whether the identified transcriptomic signatures implied greater risk for MDD varied depending on whether the brain and gene were positively versus negatively correlated. For example, if the gene and brain LVs were positively correlated, MDD risk would be estimated as a conjunction of MDD_low genes with negative BSRs and MDD_high genes with positive BSRs observed in the original data relative to the null distribution.

Control analyses: AD-relevant transcriptomic signature. The very low number (=4) of AD risk genes in the thresholded (BSR > 4) left-hemispheric gene data prevented us from running any control analyses relevant to the transcriptomic signature of AD. For the analyses

using bi-hemispheric data, we found no evidence of a statistically significant link between the AD-relevant transcriptomic profile and either of the two identified brain LVs (*p*s > .07).

Receptor Density Maps: DA, GABA, GLU, HT

To estimate receptor density maps for our neurotransmitters of interest (DA, GABA, GLU, HT), we used the normative atlas put together by [58], which is based on positron emission tomography (PET) data from over 1200 healthy individuals. Group-averaged pre-processed PET images corresponding to each tracer map for DA, GABA, GLU, HT were downloaded from https://github.com/netneurolab/hansen_receptors/tree/main/data/PET_nifti_images. Each tracer map was parcellated in the MNI-152 space based on the Schaefer atlas using the "Parcellater" function from neuromaps https://github.com/netneurolab/neuromaps/tree/main/neuromaps. Following the strategy from [58], an adapted version of the "make_receptor_matrix.py" script (https://github.com/netneurolab/hansen_receptors/tree/main/code) was employed to estimate the weighted average of the receptor density maps corresponding to each neurotransmitter of interest. This was done separately for each tracer based on the number of participants in the respective study (see Table 1 in [58]).

Each receptor density measure was standardised across all the parcels in the Schaefer atlas. The multiple indices of DA and HT receptor density were moderately to strongly correlated (DA [D1/D2]: *r* of .52; HT: *r*s from .28 to .57). Consequently, a global index of DA (combined D1/D2) and HT, respectively, receptor density was computed by averaging the standardised scores of the corresponding indices. A parcel-specific E/I measure was created by subtracting the GABA receptor density standardised score from the GLU receptor density standardised score. Brain regions with higher values on this index show relatively greater GLU (compared to GABA) receptor density.

566 **Control Variables**

567 To characterise the underpinnings of resilience in relation to the total number of acute
568 stressful experiences, we controlled for chronic exposure to material deprivation, family
569 conflict and neighbourhood crime, all of which had been shown to impact inhibitory control,
570 incentive processing and susceptibility to psychopathology.

571 **Residualisation**

572 The non-imaging variables were residualised for the following confounders:
573 (1) chronological age in order to estimate accelerated/decelerated development;
574 (1) biological sex (coded as "1" for females, "0" for males);
575 (2) handedness (coded as "0" for right-handedness and "1" for non-right-handedness);
576 (3) serious medical problems, which was based on the ABCD Parent Medical History
577 Questionnaire and computed as an average of unplanned hospital visits in the prior year for
578 chronic health conditions, head trauma, loss of consciousness and/or convulsions/trauma;
579 (4) scanner site (21 dummy variables to account for scanner-related differences, as well as
580 broad differences in family education and socio-economic status across sites);
581 (5) material deprivation, family conflict and neighbourhood crime;
582 (6) average modality-specific motion per participant (151);
583 (7) difference (in months) between the baseline and two-year follow-up sessions (only for the
584 non-imaging variables involved in longitudinal comparisons).

585 Because the difficulty of the MID and SST trials was dynamically adjusted to
586 maintain a set accuracy level (26), we saw no reason to control for behavioural performance.

587 **Data reduction: Multivariate normality.** Because the multiple linear regression
588 analyses used for confounder residualisation are sensitive to violations of multivariate
589 normality, a square-root transformation was applied to the Total Problem scores (which
590 contributes to the psychological resilience index) and the APOE-based AD PRS scores prior

591 to any analyses. Subsequently, an examination of the PRSs, resilience and accelerated
592 biological aging residuals based on the normal Q-Q plots and the Kolmogorov-Smirnov test
593 (with the Lilliefors significance correction) confirmed the multivariate normality of all non-
594 imaging variables under scrutiny.

595 **fMRI and PRS Data Analysis**

596 **Partial least squares analysis (PLS).** Partial least squares correlation (i.e., PLS), a
597 multivariate data-driven manner technique which can identify relationships between neural
598 patterns (latent variables or LVs) and individual differences variables (behavioural PLS), was
599 used to probe the transcriptomic and functional brain profiles linked to AD/MDD-related
600 genetic vulnerability, psychological resilience and accelerated biological ageing.
601 Two sets of behavioural PLS analyses were conducted. The sole analysis in the first set
602 featured resilience, biological ageing, as well as the MDD and AD (APOE- vs non-APOE-
603 based) PRSs in the "behavioural" matrix. The brain matrix contained the flexibility indices
604 estimated in NCT and modelled as four separate conditions reflecting functional brain
605 reorganisation, longitudinally within each task (incentive vs inhibitory control), as well as
606 between the two tasks at baseline and the two-year follow-up, respectively. The second set of
607 PLS analyses sought to characterise the transcriptomic signature of resilience, biological
608 ageing and AD/MDD genetic vulnerability. Specifically, it estimated the correlation between
609 the brain LVs identified in behavioural PLS analysis 1 and the parcel x gene expression level
610 matrix derived with the abagen toolbox from the comprehensive transcriptomic maps
611 provided by the Allen Brain Institute.

612 ***Significance and reliability testing*.** In all the reported PLS analyses, the significance
613 of each LV was determined using a permutation test (5000 permutations for the brain-
614 [behavior] analyses and 100,000 permutations for all the analyses involving gene expression
615 data). In the gene-brain PLS analysis, to account for correlated gene expression patterns

based on anatomical proximity we used Vasa's "rotate_parcellation" function in Matlab (https://github.com/frantisekvasa/rotate_parcellation/commit/bb8b0ef10980f162793cc180cef371e83655c505) in order to generate 100,000 spatially constrained permutations of the Schaefer brain LV, as identified in behavioral PLS analysis 1. These spatially constrained permuted brain LVs were used to assess the significance of the extracted gene LVs.

The reliability of each parcel's contribution to a particular LV was tested by submitting all weights to a bootstrap estimation (1000 bootstraps for the brain-[behaviour] analyses and 100000 bootstraps for all the analyses involving gene expression data) of the standard errors (SEs) A bootstrap ratio (BSR) (weight/SE) of at least 3 in absolute value (approximate associated p-value < .005) was used as a threshold for identifying those parcels that made a significant contribution to the identified LVs. For the gene PLS analyses, we focused on approximately the top 10% of absolute value BSRs (i.e., ~4, associated *p*-value < 10^{-4}).

Mediation analyses. To test whether perinatal adversity and/or accelerated biological ageing modulate the neurodevelopmental correlates of resilience as a function of genetic risk for AD and MDD, we conducted two moderated mediation analyses using Hayes' PROCESS 3.5 macro for SPSS. These analyses were based on the PLS results and, as such, for AD, they only involved the no-APOE-based PRS. Two simple mediation analyses involving the same predictors, mediators and outcome were also performed for exploratory purposes.

635 **Acknowledgments**. Data used in the preparation of this article were obtained from the
636 Adolescent Brain Cognitive Development (ABCD) Study (https://abcdstudy.org), held in the
637 NIMH Data Archive (NDA). This is a multisite, longitudinal study designed to recruit more
638 than 10,000 children age 9-10 and follow them over 10 years into early adulthood. The
639 ABCD Study is supported by the National Institutes of Health and additional federal partners
640 under award numbers U01DA041048, U01DA050989, U01DA051016, U01DA041022,
641 U01DA051018, U01DA051037, U01DA050987, U01DA041174, U01DA041106,
642 U01DA041117, U01DA041028, U01DA041134, U01DA050988, U01DA051039,
643 U01DA041156, U01DA041025, U01DA041120, U01DA051038, U01DA041148,
644 U01DA041093, U01DA041089, U24DA041123, U24DA041147. A full list of supporters is
645 available at https://abcdstudy.org/federal-partners.html. A listing of participating
646 sites and a complete listing of the study investigators can be found at
647 https://abcdstudy.org/consortium_members/. ABCD consortium investigators designed and
648 implemented the study and/or provided data but did not participate in analysis or writing of
649 this report. This manuscript reflects the views of the authors and may not reflect the opinions
650 or views of the NIH or ABCD consortium investigators. The authors would like to thank
651 Valentina Escott-Price for advice on the polygenic risk analyses.

652 **Materials & Correspondence.** Correspondence and material requests should be addressed to
653 R.P. (petricanr@cardiff.ac.uk).

654 **Data statement.** The raw data are available at https://nda.nih.gov/abcd upon completion of
655 the relevant data use agreements. The ABCD data repository grows and changes over time.
656 The ABCD data used in this report came from Adolescent Brain Cognitive Development
657 Study (ABCD) - Annual Release 4.0 #1299. DOIs can be found at
658 http://dx.doi.org/10.15154/1523041

659 **Code availability.** We used already existing code, as specified in the main text with links for

660 free download.

661

References

1. Alvarez-Dominguez, J. R., & Melton, D. A. (2022). Cell maturation: Hallmarks, triggers, and manipulation. *Cell, 185*, 235–249.
2. Lopez, M., Ruiz, M. O., Rovnaghi, C. R., Tam, G. K., Hiscox, J., Gotlib, I. H., Barr, D. A., Carrion, V. G., & Anand, K. (2021). The social ecology of childhood and early life adversity. *Pediatric Research, 89*, 353–367.
3. Solmi, M., Radua, J., Olivola, M., Croce, E., Soardo, L., Salazar de Pablo, G., Il Shin, J., Kirkbride, J. B., Jones, P., Kim, J. H., Kim, J. Y., Carvalho, A. F., Seeman, M. V., Correll, C. U., & Fusar-Poli, P. (2022). Age at onset of mental disorders worldwide: large-scale meta-analysis of 192 epidemiological studies. *Molecular Psychiatry, 27*, 281–295.
4. Akarca, D., Vértes, P. E., Bullmore, E. T., CALM team, & Astle, D. E. (2021). A generative network model of neurodevelopmental diversity in structural brain organization. *Nature Communications, 12*, 4216.
5. Tozzi, L., Staveland, B., Holt-Gosselin, B., Chesnut, M., Chang, S.E., Choi, D., Shiner, M.L., Wu, H., Lerma-Usabiaga, G., Sporns, O., Barch, D., Gotlib, I.H., Hastie, T.J., Kerr, A.B., Poldrack, R.A., Wandell, B.A., Wintermark, M., & Williams, L.M. (2020). The human connectome project for disordered emotional states: Protocol and rationale for a research domain criteria study of brain connectivity in young adult anxiety and depression. NeuroImage, 124, 116715.
6. Bach, A. M., Xie, W., Piazzoli, L., Jensen, S., Afreen, S., Haque, R., Petri, W. A., & Nelson, C. A. (2022). Systemic inflammation during the first year of life is associated with brain functional connectivity and future cognitive outcomes. *Developmental Cognitive Neuroscience, 53*, 101041.

687 7. Toenders, Y. J., Laskaris, L., Davey, C. G., Berk, M., Milaneschi, Y., Lamers, F.,
688 Penninx, B., & Schmaal, L. (2022). Inflammation and depression in young people: a
689 systematic review and proposed inflammatory pathways. *Molecular Psychiatry, 27*,
690 315–327.
691 8. Guerrero, A., De Strooper, B., & Arancibia-Cárcamo, I. L. (2021). Cellular senescence
692 at the crossroads of inflammation and Alzheimer's disease. *Trends in Neurosciences*,
693 S0166-2236(21)00119-3. Advance online publication.
694 https://doi.org/10.1016/j.tins.2021.06.007
695 9. Brouwer, R. M., Klein, M., Grasby, K. L., Schnack, H. G., Jahanshad, N., Teeuw, J.,
696 Thomopoulos, S. I., Sprooten, E., Franz, C. E., Gogtay, N., Kremen, W. S., Panizzon,
697 M. S., Olde Loohuis, L. M., Whelan, C. D., Aghajani, M., Alloza, C., Alnæs, D.,
698 Artiges, E., Ayesa-Arriola, R., Barker, G. J., … Hulshoff Pol, H. E. (2022). Genetic
699 variants associated with longitudinal changes in brain structure across the lifespan.
700 *Nature Neuroscience*, *25*, 421–432.
701 10. Dafsari, F.S. & Jessen, F. (2020) Depression—an underrecognized target for prevention
702 of dementia in Alzheimer's disease. *Translational Psychiatry, 10*, 160.
703 11. Lutz, M. W., Luo, S., Williamson, D. E., & Chiba-Falek, O. (2020). Shared genetic
704 etiology underlying late-onset Alzheimer's disease and posttraumatic stress syndrome.
705 *Alzheimer's & Dementia : The journal of the Alzheimer's Association, 16*, 1280–1292.
706 12. De Jager, C. H., White, C. C., Bennett, D. A., & Ma, Y. (2021). Neuroticism alters the
707 transcriptome of the frontal cortex to contribute to the cognitive decline and onset of
708 Alzheimer's disease. *Translational Psychiatry, 11*, 139.
709 13. Harerimana, N. V., Liu, Y., Gerasimov, E. S., Duong, D., Beach, T. G., Reiman, E. M.,
710 Schneider, J. A., Boyle, P., Lori, A., Bennett, D. A., Lah, J. J., Levey, A. I., Seyfried, N.

T., Wingo, T. S., & Wingo, A. P. (2022). Genetic Evidence Supporting a Causal Role of Depression in Alzheimer's Disease. *Biological Psychiatry, 92*, 25–33.

14. Ho, T. C., & King, L. S. (2021). Mechanisms of neuroplasticity linking early adversity to depression: developmental considerations. *Translational Psychiatry, 11*, 517.
15. De Strooper, B., & Karran, E. (2016). The Cellular Phase of Alzheimer's Disease. *Cell, 164*, 603–615.
16. Frisoni, G. B., Altomare, D., Thal, D. R., Ribaldi, F., van der Kant, R., Ossenkoppele, R., Blennow, K., Cummings, J., van Duijn, C., Nilsson, P. M., Dietrich, P. Y., Scheltens, P., & Dubois, B. (2022). The probabilistic model of Alzheimer disease: the amyloid hypothesis revised. *Nature Reviews. Neuroscience, 23*, 53–66.
17. Kalisch, R., Cramer, A., Binder, H., Fritz, J., Leertouwer, I., Lunansky, G., Meyer, B., Timmer, J., Veer, I. M., & van Harmelen, A. L. (2019). Deconstructing and Reconstructing Resilience: A Dynamic Network Approach. *Perspectives on Psychological Science, 14*, 765–777.
18. Gee, D. G. (2021). Early Adversity and Development: Parsing Heterogeneity and Identifying Pathways of Risk and Resilience. *The American Journal of Psychiatry, 178*, 998–1013.
19. Coley, E., & Hsiao, E. Y. (2021). Malnutrition and the microbiome as modifiers of early neurodevelopment. *Trends in Neurosciences, 44*, 753–764.
20. Krontira, A. C., Cruceanu, C., & Binder, E. B. (2020). Glucocorticoids as Mediators of Adverse Outcomes of Prenatal Stress. *Trends in Neurosciences, 43*, 394–405.
21. Mareckova, K., Marecek, R., Andryskova, L., Brazdil, M., & Nikolova, Y. S. (2020). Maternal Depressive Symptoms During Pregnancy and Brain Age in Young Adult Offspring: Findings from a Prenatal Birth Cohort. *Cerebral Cortex, 30*, 3991–3999.

735 22. Merhar, S. L., Jiang, W., Parikh, N. A., Yin, W., Zhou, Z., Tkach, J. A., Wang, L.,
736 Kline-Fath, B. M., He, L., Braimah, A., Vannest, J., & Lin, W. (2021). Effects of
737 prenatal opioid exposure on functional networks in infancy. Developmental Cognitive
738 Neuroscience, 51, 100996.
739 23. Stephen, J. M., Hill, D. E., & Candelaria-Cook, F. T. (2021). Examining the effects of
740 prenatal alcohol exposure on corticothalamic connectivity: A multimodal neuroimaging
741 study in children. *Developmental Cognitive Neuroscience, 52*, 101019.
742 24. Thomason, M. E., Palopoli, A. C., Jariwala, N. N., Werchan, D. M., Chen, A., Adhikari,
743 S., Espinoza-Heredia, C., Brito, N. H., & Trentacosta, C. J. (2021). Miswiring the brain:
744 Human prenatal Δ9-tetrahydrocannabinol use associated with altered fetal hippocampal
745 brain network connectivity. Developmental Cognitive Neuroscience, 51, 101000.
746 25. Zutshi, I., Gupta, S., Zanoletti, O., Sandi, C., & Poirier, G. L. (2021). Early life adoption
747 shows rearing environment supersedes transgenerational effects of paternal stress on
748 aggressive temperament in the offspring. *Translational Psychiatry, 11*, 533.
749 26. Casey, B. J., Cannonier, T., Conley, M. I., Cohen, A. O., Barch, D. M., Heitzeg, M. M.,
750 Soules, M. E., Teslovich, T., Dellarco, D. V., Garavan, H., Orr, C. A., Wager, T. D.,
751 Banich, M. T., Speer, N. K., Sutherland, M. T., Riedel, M. C., Dick, A. S., Bjork, J. M.,
752 Thomas, K. M., Chaarani, B., … ABCD Imaging Acquisition Workgroup (2018). The
753 Adolescent Brain Cognitive Development (ABCD) study: Imaging acquisition across 21
754 sites. *Developmental Cognitive Neuroscience*, *32*, 43–54.
755 27. Fornito, A., Zalesky, A., Breakspear, M. J. (2015). The connectomics of brain disorders.
756 *Nature Reviews Neuroscience, 16,* 159-172.
757 28. Váša, F., Romero-Garcia, R., Kitzbichler, M. G., Seidlitz, J., Whitaker, K. J., Vaghi, M.
758 M., Kundu, P., Patel, A. X., Fonagy, P., Dolan, R. J., Jones, P. B., Goodyer, I. M.,
759 NSPN Consortium, Vértes, P. E., & Bullmore, E. T. (2020). Conservative and disruptive

760 modes of adolescent change in human brain functional connectivity. Proceedings of the
761 National Academy of Sciences of the United States of America, 117, 3248–3253.
762 29. Young, A. I., Benonisdottir, S., Przeworski, M., & Kong, A. (2019). Deconstructing the
763 sources of genotype-phenotype associations in humans. *Science*, *365*, 1396–1400.
764 30. Kunkle, B. W., Grenier-Boley, B., Sims, R., Bis, J. C., Damotte, V., Naj, A. C et al.
765 (2019). Genetic meta-analysis of diagnosed Alzheimer's disease identifies new risk loci
766 and implicates Aβ, tau, immunity and lipid processing. *Nature genetics*, *51*, 414–430.
767 31. Howard, D. M., Adams, M. J., Clarke, T. K., Hafferty, J. D., Gibson, J., Shirali, M. et al.
768 (2019). Genome-wide meta-analysis of depression identifies 102 independent variants
769 and highlights the importance of the prefrontal brain regions. *Nature neuroscience*, *22*,
770 343–352.
771 32. Cao, Z., Ottino-Gonzalez, J., Cupertino, R. B., Juliano, A., Chaarani, B., Banaschewski,
772 T., Bokde, A., Quinlan, E. B., Desrivières, S., Flor, H., Grigis, A., Gowland, P., Heinz,
773 A., Brühl, R., Martinot, J. L., Martinot, M. P., Artiges, E., Nees, F., Orfanos, D. P.,
774 Paus, T., … IMAGEN consortiu (2021). Characterizing reward system neural
775 trajectories from adolescence to young adulthood. *Developmental Cognitive*
776 *Neuroscience*, *52*, 101042.
777 33. Constantinidis, C., & Luna, B. (2019). Neural Substrates of Inhibitory Control
778 Maturation in Adolescence. *Trends in Neurosciences*, *42*, 604–616.
779 34. Jenkins, L. M., Kogan, A., Malinab, M., Ingo, C., Sedaghat, S., Bryan, N. R., Yaffe, K.,
780 Parrish, T. B., Nemeth, A. J., Lloyd-Jones, D. M., Launer, L. J., Wang, L., & Sorond, F.
781 (2021). Blood pressure, executive function, and network connectivity in middle-aged
782 adults at risk of dementia in late life. *Proceedings of the National Academy of Sciences*
783 *of the United States of America*, *118*, e2024265118.

784 35. Lloyd, A., McKay, R. T., & Furl, N. (2022). Individuals with adverse childhood
785 experiences explore less and underweight reward feedback. *Proceedings of the National*
786 *Academy of Sciences of the United States of America*, *119*, e2109373119.
787 36. McTeague, L.M., Huemer, J., Carreon, D.M., Jiang, Y., Eickhoff, S.B., & Etkin A.
788 (2017) Identification of common neural circuit disruptions in cognitive control across
789 psychiatric disorders. American Journal of Psychiatry, 174, 676-685.
790 37. Ng, T. H., Alloy, L. B., & Smith, D. V. (2019). Meta-analysis of reward processing in
791 major depressive disorder reveals distinct abnormalities within the reward circuit.
792 *Translational Psychiatry*, *9*, 293.
793 38. Roeckner, A. R., Oliver, K. I., Lebois, L., van Rooij, S., & Stevens, J. S. (2021). Neural
794 contributors to trauma resilience: a review of longitudinal neuroimaging studies.
795 Translational Psychiatry, 11, 508.
796 39. DiSabato, D. J., Nemeth, D. P., Liu, X., Witcher, K. G., O'Neil, S. M., Oliver, B., Bray,
797 C. E., Sheridan, J. F., Godbout, J. P., & Quan, N. (2021). Interleukin-1 receptor on
798 hippocampal neurons drives social withdrawal and cognitive deficits after chronic social
799 stress. *Molecular Psychiatry*, *26*, 4770–4782.
800 40. Englund, J., Haikonen, J., Shteinikov, V., Amarilla, S. P., Atanasova, T., Shintyapina,
801 A., Ryazantseva, M., Partanen, J., Voikar, V., & Lauri, S. E. (2021). Downregulation of
802 kainate receptors regulating GABAergic transmission in amygdala after early life stress
803 is associated with anxiety-like behavior in rodents. *Translational Psychiatry*, *11*, 538.
804 41. Fogaça, M. V., Wu, M., Li, C., Li, X. Y., Picciotto, M. R., & Duman, R. S. (2021).
805 Inhibition of GABA interneurons in the mPFC is sufficient and necessary for rapid
806 antidepressant responses. *Molecular Psychiatry*, *26*, 3277–3291.
807 42. Fox, M. E., & Lobo, M. K. (2019). The molecular and cellular mechanisms of
808 depression: a focus on reward circuitry. *Molecular Psychiatry, 24*, 1798–1815.

809 43. Joffe, M. E., Maksymetz, J., Luschinger, J. R., Dogra, S., Ferranti, A. S., Luessen, D. J.,
810 Gallinger, I. M., Xiang, Z., Branthwaite, H., Melugin, P. R., Williford, K. M., Centanni,
811 S. W., Shields, B. C., Lindsley, C. W., Calipari, E. S., Siciliano, C. A., Niswender, C.
812 M., Tadross, M. R., Winder, D. G., & Conn, P. J. (2022). Acute restraint stress redirects
813 prefrontal cortex circuit function through mGlu5 receptor plasticity on somatostatin-
814 expressing interneurons. *Neuron*, S0896-6273(21)01044-8.
815 44. Karalija, N., Köhncke, Y., Düzel, S., Bertram, L., Papenberg, G., Demuth, I., Lill, C.
816 M., Johansson, J., Riklund, K., Lövdén, M., Bäckman, L., Nyberg, L., Lindenberger, U.,
817 & Brandmaier, A. M. (2021). A common polymorphism in the dopamine transporter
818 gene predicts working memory performance and in vivo dopamine integrity in aging.
819 *NeuroImage*, *245*, 118707.
820 45. Kim J., Kang S., Choi T.-Y., Chang K.-A & Koo J.W. (2022) Metabotropic glutamate
821 receptor 5 in amygdala target neurons regulates susceptibility to chronic social stress,
822 *Biological Psychiatry*, doi: https://doi.org/10.1016/j.biopsych.2022.01.006.
823 46. Svensson, J. E., Svanborg, C., Plavén-Sigray, P., Kaldo, V., Halldin, C., Schain, M., &
824 Lundberg, J. (2021). Serotonin transporter availability increases in patients recovering
825 from a depressive episode. *Translational Psychiatry, 11*, 264.
826 47. Westbrook, A., Frank, M. J., & Cools, R. (2021). A mosaic of cost-benefit control over
827 cortico-striatal circuitry. *Trends in Cognitive Sciences*, *25*, 710–721.
828 48. Yan, Z., & Rein, B. (2022). Mechanisms of synaptic transmission dysregulation in the
829 prefrontal cortex: pathophysiological implications. *Molecular Psychiatry, 27*, 445–465.
830 49. Zhong, P., Cao, Q., & Yan, Z. (2022). Selective impairment of circuits between
831 prefrontal cortex glutamatergic neurons and basal forebrain cholinergic neurons in a
832 tauopathy mouse model. *Cerebral Cortex*, bhac036. Advance online publication.
833 https://doi.org/10.1093/cercor/bhac036

834 50. Mucha, P. J., Richardson, T., Macon, K., Porter, M. A., & Onnela, J. P. (2010).
835 Community structure in time-dependent, multiscale, and multiplex
836 networks. *Science*, *328*, 876–878.
837 51. Schaefer, A., Kong, R., Gordon, E. M., Laumann, T. O., Zuo, X. N., Holmes, A. J.,
838 Eickhoff, S. B., & Yeo, B. (2018). Local-Global Parcellation of the Human Cerebral
839 Cortex from Intrinsic Functional Connectivity MRI. *Cerebral Cortex*, *28*, 3095–3114.
840 52. Bassett, D.S. [2017, November]. Network Community Toolbox. Retrieved from
841 http://commdetect.weebly.com/
842 53. Finc, K., Bonna, K., He, X., Lydon-Staley, D. M., Kühn, S., Duch, W., & Bassett, D. S.
843 (2020). Dynamic reconfiguration of functional brain networks during working memory
844 training. *Nature Communications*, *11*, 2435.
845 54. Nougaret, S., Baunez, C., & Ravel, S. (2022). Neurons in the monkey's subthalamic
846 nucleus differentially encode motivation and effort. *The Journal of Neuroscience*, JN-
847 RM-0281-21. Advance online publication. https://doi.org/10.1523/JNEUROSCI.0281-
848 21.2021
849 55. Petrican, R., & Grady, C. L. (2017). Contextual and Developmental Differences in the
850 Neural Architecture of Cognitive Control. *The Journal of Neuroscience*, *37*, 7711–7726.
851 56. Reineberg, A. E., Banich, M. T., Wager, T. D., & Friedman, N. P. (2022). Context-
852 specific activations are a hallmark of the neural basis of individual differences in
853 general executive function. *NeuroImage*, *249*, 118845.
854 57. Markello, R. D., Arnatkeviciute, A., Poline, J. B., Fulcher, B. D., Fornito, A., & Misic,
855 B. (2021). Standardizing workflows in imaging transcriptomics with the abagen
856 toolbox. *eLife*, *10*, e72129.
857 58. Hansen, JY, Shafiei G, Markello, RD, Smart, K, Cox, SML, Wu, Y, Gallezot, J-D,
858 Aumont, E, Servaes, S, Scala, SG, DuBois, JM, Wainstein, G, Bezgin, G, Funck, T,

Schmitz, TW, Spreng, RN, Soucy, J-P, Baillet, S, Guimond, S, Hietala, J, Bédard, M-A, Leyton, M, Kobayashi, E, Rosa-Neto, P, Palomero-Gallagher, N, Shine, JM, Carson, RE, Tuominen, L, Dagher A, & Misic B (2021). Mapping neurotransmitter systems to the structural and functional organization of the human neocortex. *Biorxiv*. doi:10.1101/2021.10.28.466336.

59. Arnatkeviciute, A., Fulcher, B. D., Bellgrove, M. A., & Fornito, A. (2021). Where the genome meets the connectome: Understanding how genes shape human brain connectivity. *NeuroImage, 244*, 118570.

60. Qi, G., Zhang, P., Li, T., Li, M., Zhang, Q., He, F., Zhang, L., Cai, H., Lv, X., Qiao, H., Chen, X., Ming, J., & Tian, B. (2022). NAc-VTA circuit underlies emotional stress-induced anxiety-like behavior in the three-chamber vicarious social defeat stress mouse model. Nature Communications, 13, 577.

61. Javaheripour, N., Li, M., Chand, T., Krug, A., Kircher, T., Dannlowski, U., Nenadić, I., Hamilton, J. P., Sacchet, M. D., Gotlib, I. H., Walter, H., Frodl, T., Grimm, S., Harrison, B. J., Wolf, C. R., Olbrich, S., van Wingen, G., Pezawas, L., Parker, G., Hyett, M. P., … Wagner, G. (2021). Altered resting-state functional connectome in major depressive disorder: a mega-analysis from the PsyMRI consortium. *Translational Psychiatry, 11*, 511.

62. Kebets, V., Holmes, A. J., Orban, C., Tang, S., Li, J., Sun, N., Kong, R., Poldrack, R. A., & Yeo, B. (2019). Somatosensory-motor dysconnectivity spans multiple transdiagnostic dimensions of psychopathology. *Biological Psychiatry, 86*, 779–791.

63. Eck, S. R., & Bangasser, D. A. (2020). The effects of early life stress on motivated behaviors: A role for gonadal hormones. *Neuroscience and Biobehavioral Reviews, 119*, 86–100.

883 64. Jacobs, E. G., & Goldstein, J. M. (2018). The Middle-Aged Brain: Biological sex and
884 sex hormones shape memory circuitry. *Current Opinion in Behavioral Sciences, 23*, 84-
885 91.
886 65. Peper, J. S., & Dahl, R. E. (2013). Surging Hormones: Brain-Behavior Interactions
887 During Puberty. *Current Directions in Psychological Science, 22*, 134–139.
888 66. Knoedler, J. R., Inoue, S., Bayless, D. W., Yang, T., Tantry, A., Davis, C. H., Leung, N.
889 Y., Parthasarathy, S., Wang, G., Alvarado, M., Rizvi, A. H., Fenno, L. E.,
890 Ramakrishnan, C., Deisseroth, K., & Shah, N. M. (2022). A functional cellular
891 framework for sex and estrous cycle-dependent gene expression and behavior. *Cell, 185*,
892 654–671.e22.
893 67. Mueller, J. M., Pritschet, L., Santander, T., Taylor, C. M., Grafton, S. T., Jacobs, E. G.,
894 & Carlson, J. M. (2021). Dynamic community detection reveals transient reorganization
895 of functional brain networks across a female menstrual cycle. *Network Neuroscience, 5*,
896 125–144.
897 68. Ray, D., Bezmaternykh, D., Mel'nikov, M., Friston, K. J., & Das, M. (2021). Altered
898 effective connectivity in sensorimotor cortices is a signature of severity and clinical
899 course in depression. Proceedings of the National Academy of Sciences of the United
900 States of America, 118, e2105730118.
901 69. Kalemaki, K., Velli, A., Christodoulou, O., Denaxa, M., Karagogeos, D., &
902 Sidiropoulou, K. (2021). The Developmental Changes in Intrinsic and Synaptic
903 Properties of Prefrontal Neurons Enhance Local Network Activity from the Second to
904 the Third Postnatal Weeks in Mice. Cerebral Cortex, bhab438. Advance online
905 publication. https://doi.org/10.1093/cercor/bhab438

906 70. McGovern, D. J., Polter, A. M., & Root, D. H. (2021). Neurochemical Signaling of
907 Reward and Aversion to Ventral Tegmental Area Glutamate Neurons. *The Journal of*
908 *Neuroscience, 41*, 5471–5486.
909 71. Al-Hasani, R., Gowrishankar, R., Schmitz, G. P., Pedersen, C. E., Marcus, D. J.,
910 Shirley, S. E., Hobbs, T. E., Elerding, A. J., Renaud, S. J., Jing, M., Li, Y., Alvarez, V.
911 A., Lemos, J. C., & Bruchas, M. R. (2021). Ventral tegmental area GABAergic
912 inhibition of cholinergic interneurons in the ventral nucleus accumbens shell promotes
913 reward reinforcement. *Nature Neuroscience, 24*, 1414–1428.
914 72. Stephenson-Jones, M., Bravo-Rivera, C., Ahrens, S., Furlan, A., Xiao, X., Fernandes-
915 Henriques, C., & Li, B. (2020). Opposing Contributions of GABAergic and
916 Glutamatergic Ventral Pallidal Neurons to Motivational Behaviors. *Neuron, 105*, 921–
917 933.e5.
918 73. Ferrara, N. C., Trask, S., Avonts, B., Loh, M. K., Padival, M., & Rosenkranz, J. A.
919 (2021). Developmental Shifts in Amygdala Activity during a High Social Drive State.
920 The *Journal of Neuroscience, 41*, 9308–9325.
921 74. Min, J., Nashiro, K., Yoo, H. J., Cho, C., Nasseri, P., Bachman, S. L., Porat, S., Thayer,
922 J. F., Chang, C., Lee, T. H., & Mather, M. (2022). Emotion Downregulation Targets
923 Interoceptive Brain Regions While Emotion Upregulation Targets Other Affective Brain
924 Regions. The Journal of Neuroscience, 42, 2973–2985.
925 75. Daselaar, S. M., Rice, H. J., Greenberg, D. L., Cabeza, R., LaBar, K. S., & Rubin, D. C.
926 (2008). The spatiotemporal dynamics of autobiographical memory: neural correlates of
927 recall, emotional intensity, and reliving. *Cerebral Cortex, 18*, 217–229.
928 76. Huijbers, W., Pennartz, C. M., Rubin, D. C., & Daselaar, S. M. (2011). Imagery and
929 retrieval of auditory and visual information: neural correlates of successful and
930 unsuccessful performance. *Neuropsychologia, 49*, 1730–1740.

931 77. Bellenguez, C., Küçükali, F., Jansen, I. E., Kleineidam, L., Moreno-Grau, S., Amin, N.,
932 Naj, A. C., Campos-Martin, R., Grenier-Boley, B., Andrade, V., Holmans, P. A.,
933 Boland, A., Damotte, V., van der Lee, S. J., Costa, M. R., Kuulasmaa, T., Yang, Q., de
934 Rojas, I., Bis, J. C., Yaqub, A., … Lambert, J. C. (2022). New insights into the genetic
935 etiology of Alzheimer's disease and related dementias. *Nature Genetics*, *54*, 412–436.
936 78. Brivio, P., Audano, M., Gallo, M. T., Gruca, P., Lason, M., Litwa, E., Fumagalli, F.,
937 Papp, M., Mitro, N., & Calabrese, F. (2022). Metabolomic signature and mitochondrial
938 dynamics outline the difference between vulnerability and resilience to chronic stress.
939 *Translational Psychiatry*, *12*, 87.
940 79. Cathomas, F., Holt, L. M., Parise, E. M., Liu, J., Murrough, J. W., Casaccia, P., Nestler,
941 E. J., & Russo, S. J. (2022). Beyond the neuron: Role of non-neuronal cells in stress
942 disorders. *Neuron*, S0896-6273(22)00102-7. Advance online publication.
943 https://doi.org/10.1016/j.neuron.2022.01.033
944 80. Cheng, X. T., Huang, N., & Sheng, Z. H. (2022). Programming axonal mitochondrial
945 maintenance and bioenergetics in neurodegeneration and regeneration. *Neuron*, S0896-
946 6273(22)00251-3. Advance online publication.
947 https://doi.org/10.1016/j.neuron.2022.03.015
948 81. Mederos, S., Sánchez-Puelles, C., Esparza, J., Valero, M., Ponomarenko, A., & Perea,
949 G. (2021). GABAergic signaling to astrocytes in the prefrontal cortex sustains goal-
950 directed behaviors. Nature Neuroscience, 24, 82–92.
951 82. Wightman, D. P., Jansen, I. E., Savage, J. E., Shadrin, A. A., Bahrami, S., Holland, D.,
952 Rongve, A., Børte, S., Winsvold, B. S., Drange, O. K., Martinsen, A. E., Skogholt, A.
953 H., Willer, C., Bråthen, G., Bosnes, I., Nielsen, J. B., Fritsche, L. G., Thomas, L. F.,
954 Pedersen, L. M., Gabrielsen, M. E., … Posthuma, D. (2021). A genome-wide

955 association study with 1,126,563 individuals identifies new risk loci for Alzheimer's
956 disease. *Nature Genetics, 53,* 1276–1282.
957 83. Gal, S., Coldham, Y., Tik, N., Bernstein-Eliav, M., & Tavor, I. (2022) Act natural:
958 Functional connectivity from naturalistic stimuli fMRI outperforms resting-state in
959 predicting brain activity. *NeuroImage,* doi:
960 https://doi.org/10.1016/j.neuroimage.2022.119359
961 84. Chen, J., Tam, A., Kebets, V., Orban, C., Ooi, L., Asplund, C. L., Marek, S.,
962 Dosenbach, N., Eickhoff, S. B., Bzdok, D., Holmes, A. J., & Yeo, B. (2022). Shared and
963 unique brain network features predict cognitive, personality, and mental health scores in
964 the ABCD study. *Nature Communications, 13,* 2217.
965 85. Gu, Z., Jamison, K. W., Sabuncu, M. R., & Kuceyeski, A. (2021). Heritability and
966 interindividual variability of regional structure-function coupling. *Nature*
967 *Communications, 12,* 4894.
968 86. Huang, H., Zheng, S., Yang, Z., Wu, Y., Li, Y., Qiu, J., Cheng, Y., Lin, P., Lin, Y.,
969 Guan, J., Mikulis, D. J., Zhou, T., & Wu, R. (2022). Voxel-based morphometry and a
970 deep learning model for the diagnosis of early Alzheimer's disease based on cerebral
971 gray matter changes. *Cerebral Cortex,* bhac099. Advance online publication.
972 https://doi.org/10.1093/cercor/bhac099
973 87. Lu, F., Cui, Q., Chen, Y., He, Z., Sheng, W., Tang, Q., Yang, Y., Luo, W., Yu, Y.,
974 Chen, J., Li, D., Deng, J., Zeng, Y., & Chen, H. (2022). Insular-associated causal
975 network of structural covariance evaluating progressive gray matter changes in major
976 depressive disorder. Cerebral Cortex, bhac105. Advance online publication.
977 https://doi.org/10.1093/cercor/bhac105
978 88. Zhao, B., Zhang, J., Ibrahim, J. G., Luo, T., Santelli, R. C., Li, Y., Li, T., Shan, Y., Zhu,
979 Z., Zhou, F., Liao, H., Nichols, T. E., & Zhu, H. (2021). Large-scale GWAS reveals

980 genetic architecture of brain white matter microstructure and genetic overlap with
981 cognitive and mental health traits (n = 17,706). *Molecular Psychiatry, 26*, 3943–3955.
982 89. Simpson, E. H., Gallo, E. F., Balsam, P. D., Javitch, J. A., & Kellendonk, C. (2022).
983 How changes in dopamine D2 receptor levels alter striatal circuit function and
984 motivation. Molecular Psychiatry, 27, 436–444.
985 90. Mei, J., Muller, E., & Ramaswamy, S. (2022). Informing deep neural networks by
986 multiscale principles of neuromodulatory systems. Trends in Neurosciences, 45, 237–
987 250.
988 91. Caradonna, S. G., Einhorn, N. R., Saudagar, V., Khalil, H., Petty, G. H., Lihagen, A.,
989 LeFloch, C., Lee, F. S., Akil, H., Guidotti, A., McEwen, B. S., Gatta, E., & Marrocco, J.
990 (2022). Corticosterone induces discrete epigenetic signatures in the dorsal and ventral
991 hippocampus that depend upon sex and genotype: focus on methylated Nr3c1 gene.
992 *Translational Psychiatry*, 12, 109.
993 92. Kuhn, L., Noack, H., Wagels, L., Prothmann, A., Schulik, A., Aydin, E., Nieratschker,
994 V., Derntl, B., & Habel, U. (2022). Sex-dependent multimodal response profiles to
995 psychosocial stress. *Cerebral Cortex*, bhac086. Advance online publication.
996 https://doi.org/10.1093/cercor/bhac086
997 93. Bernabeu, E., Canela-Xandri, O., Rawlik, K., Talenti, A., Prendergast, J., & Tenesa, A.
998 (2021). Sex differences in genetic architecture in the UK Biobank. *Nature Genetics, 53*,
999 1283–1289.
1000 94. Ludyga, S., Gerber, M., & Kamijo, K. (2022). Exercise types and working memory
1001 components during development. *Trends in Cognitive Sciences, 26*, 191–203.
1002 95. Rogers, C. R., Chen, X., Kwon, S. J., McElwain, N. L., & Telzer, E. H. (2022). The role
1003 of early attachment and parental presence in adolescent behavioural and neurobiological
1004 regulation. Developmental Cognitive Neuroscience, 53, 101046.

96. Willoughby, T., Heffer, T., van Noordt, S., Desjardins, J., Segalowitz, S., & Schmidt, L. (2021). An ERP investigation of children and adolescents' sensitivity to wins and losses during a peer observation manipulation. *Developmental Cognitive Neuroscience, 51*, 100995.

97. Nosjean, A., & Granon, S. (2021). Brain Adaptation to Acute Stress: Effect of Time, Social Buffering, and Nicotinic Cholinergic System. *Cerebral Cortex*, bhab461. Advance online publication. https://doi.org/10.1093/cercor/bhab461

98. Abdellaoui, A., & Verweij, K. (2021). Dissecting polygenic signals from genome-wide association studies on human behaviour. Nature Human Behaviour, 5, 686–694.

99. Wojcik, G. L., Graff, M., Nishimura, K. K., Tao, R., Haessler, J., Gignoux, C. R., Highland, H. M., Patel, Y. M., Sorokin, E. P., Avery, C. L., Belbin, G. M., Bien, S. A., Cheng, I., Cullina, S., Hodonsky, C. J., Hu, Y., Huckins, L. M., Jeff, J., Justice, A. E., Kocarnik, J. M., … Carlson, C. S. (2019). Genetic analyses of diverse populations improves discovery for complex traits. *Nature, 570*, 514–518.

100. Barch, D. M., Albaugh, M. D., Baskin-Sommers, A., Bryant, B. E., Clark, D. B., Dick, A. S., Feczko, E., Foxe, J. J., Gee, D. G., Giedd, J., Glantz, M. D., Hudziak, J. J., Karcher, N. R., LeBlanc, K., Maddox, M., McGlade, E. C., Mulford, C., Nagel, B. J., Neigh, G., Palmer, C. E., … Xie, L. (2021). Demographic and mental health assessments in the adolescent brain and cognitive development study: Updates and age-related trajectories. *Developmental Cognitive Neuroscience, 52, 101031*.

101. Barch, D. M., Albaugh, M. D., Avenevoli, S., Chang, L., Clark, D. B., Glantz, M. D., Hudziak, J. J., Jernigan, T. L., Tapert, S. F., Yurgelun-Todd, D., Alia-Klein, N., Potter, A. S., Paulus, M. P., Prouty, D., Zucker, R. A., & Sher, K. J. (2018). Demographic, physical and mental health assessments in the adolescent brain and cognitive

development study: Rationale and description. *Developmental Cognitive Neuroscience*, *32*, 55–66.

102. Hagler DJ, Jr, Hatton, S., Cornejo, M.D., Makowski, C., Fair, D.A., Dick, A.S., Sutherland, M.T., Casey, B.J., Barch, D.M., Harms, M.P., Watts, R., Bjork, J.M., Garavan, H.P., Hilmer, L., Pung, C.J., Sicat, C.S., Kuperman, J., Bartsch, H., Xue, F., Heitzeg, M.M., Laird, A.R., Trinh, T.T., Gonzalez, R., Tapert, S.F., Riedel, M.C., Squeglia, L.M., Hyde, L.W., Rosenberg, M.D., Earl, E.A., Howlett, K.D., Baker, F.C., Soules, M., Diaz, J., de Leon, O.R., Thompson, W.K., Neale, M.C., Herting, M., Sowell, E.R., Alvarez, R.P., Hawes, S.W., Sanchez, W.K., Bodurka, J., Breslin, F.J., Morris, A.S., Paulus, M.P., Simmons, W.K., Polimeni, J.R., van der Kouwe, A., Nencka, A.S., Gray, K.M., Pierpaoli, C., Matochik, J.A., Noronha, A., Aklin, W.M., Conway, K., Glantz, M., Hoffman, E., Little, R., Lopez, M., Barch, V., Weiss, S.R., Wolff-Hughes, D.L., DelCarmen-Wiggins, R., Feldstein Ewing, S.W., MirandaDominguez, O., Nagel, B.J., Perrone, A.J., Sturgeon, D.T., Goldstone, A., Pfefferbaum, A., Pohl, K.M., Prouty, D., Uban, K., Bookheimer, S.Y., Dapretto, M., Galvan, A., Bagot, K., Giedd, J., Infante, M.A., Jacobus, J., Patrick, K., Shilling, P.D., Desikan, R., Li, Y., Sugrue, L., Banich, M.T., Friedman, N., Hewitt, J.K., Hopfer, C., Sakai, J., Tanabe, J., Cottler, L.B., Nixon, S.J., Chang, L., Cloak, C., Nagel, T., Reeves, G., Kennedy, D.N., Heeringa, S., Peltier, S., Schulenberg, J., Sripada, C., Zucker, R.A., Iacono, W.G., Luciana, M., Calabro, F.J., Clark, D.B., Lewis, D.A., Luna, B., Schirda, C., Brima, T., Foxe, J.J., Freedman, E.G., Mruzek, D.W., Mason, M. J., Huber, R., McGlade, E., Prescot, A., Renshaw, P.F., Yurgelun-Todd, D.A., Allgaier, N.A., Dumas, J.A., Ivanova, M., Potter, A., Florsheim, P., Larson, C., Lisdahl, K., Charness, M.E., Fuemmeler, B., Hettema, J.M., Maes, H.H., Florsheim, J., Anokhin, A.P., Glaser, P., Heath, A.C., Madden, P.A., Baskin-Sommers, A., Constable, R.T., Grant, S.J., Dowling,

1054 G.J., Brown, S.A., Jernigan, T.L., Dale, A.M., 2019. Image processing and analysis
1055 methods for the Adolescent Brain Cognitive Development Study. *NeuroImage, 202*,
1056 116091.